Systems & Control Transactions

**Original Research Article**
*Peer Reviewed Conference Proceeding*
ESCAPE 36 - European Symposium on Computer Aided Process Engineering
Sheffield, UK. 21-24 June 2026

PSE PRESS

# Advancing Industrial Fermentation across scales: Model Development, Cost Analysis, and Predictive Control

**Marc Lemperle[a]*, Pedram Ramin[a], Julian Kager[a], Benny Cassells[b], Stuart Stocks[b], Krist V. Gernaey[a]**

[a] Process and Systems Engineering Center (PROSYS), department of Chemical and Biochemical Engineering, Technical University of Denmark, Building 228A, 28000 Kgs. Lyngby
[b] Novonesis, Fermentation Pilot Plant, Krogshoejvej 36, 2880 Bagsværd, Denmark
* Corresponding Author: marlem@dtu.dk

## ABSTRACT

The bioprocess industry is actively exploring technologies associated with the fourth industrial revolution, with modeling offering considerable potential for process optimization. Nevertheless, model adoption in industry remains limited. This is partly because model development continues to depend heavily on offline sampling, and because relatively few industrial applications convincingly demonstrate their practical value. This study therefore first examines the benefits of online rheology and online biomass measurements for model development and demonstrates, among other aspects, that online biomass significantly improves model fidelity. The second part examines how electricity prices affect process conditions, a key factor in production, and finds that, contrary to common practice, maximizing all operating parameters is not the most cost-effective strategy. Finally, an in-silico framework for model predictive control, applied to a reactor end-fill scenario, demonstrates that oxygen-controlled processes can be dynamically optimized, highlighting the strong potential of bioprocess models for industrial usage.

**Keywords**: Bioprocess Modelling, Cost Analysis, Model Predictive Control

## INTRODUCTION

Fermentation processes are well-established biochemical operations that utilize microorganisms to produce specific compounds, ranging from monoclonal antibodies to chemicals and industrial enzymes [1]. Although individual processes differ substantially, all industrial fermentations rely on a complex interplay between the underlying biological system and its physical reactor environment [2], [3].

Accurate modeling of fermentation processes is considered a crucial step forward in the ongoing optimization, monitoring, control and scaling of such processes [4]. Nevertheless, the application and usage of such mathematical bioprocess models in industry remains limited, largely because the model development is highly resource-intensive and time-consuming [5].

A major contributor to this challenge is the reliance on offline measurements for rheological characterization and cell-weight–based analyses [6].

However, online measurement technologies are constantly emerging within industrial settings, raising the question of to what extent they can support model development and improve model accuracy from an industrial perspective [7].

For instance, rheological offline measurements are laborious and additionally require an estimate of the apparent viscosity based on numerous assumptions. This can be substituted by online measurements of the dynamic viscosity using a vibrational viscometer operating in the upper Newtonian region, in which the fluid behaves shear-independently. Dynamic viscosity is referred to in the following as online viscosity [8]. Additionally, online biomass sensors that quantify viable cells based on permittivity can replace the cumbersome and, under current industrial conditions, error-prone measurements of cell dry weight (CDW) [9], [10], [11].

This work first aims to investigate the extent to which the integration of those two online measurement technologies improves model development and enhances model accuracy for industrial fungal fermentation processes at pilot and production scale.

This is done by comparing three modeling approaches, leading to three different models, developed

using pilot plant data and validated through pilot and large-scale simulations: (i) a mechanistic model based on offline CDW and offline rheology measurements, (ii) a hybrid model combining offline CDW and online viscosity, and (iii) a hybrid model relying on online viable cell concentration and online viscosity. The complexity of the model is addressed in more detail in the "Methodology" section.

Alongside the effort required for development, the usage of models in industry may also be slowed down by a lack of practical examples that clearly demonstrate their benefits [12], [13], [14]. Therefore, the second part of this work presents two model applications tailored to an established dissolved oxygen (DO)-controlled enzyme-production process. First, a cost analysis under varying electricity prices is conducted to provide economic insights into fermentation operations. Second, an in-silico framework for predictive control is implemented to dynamically optimize DO-controlled fermentations, while ensuring a defined reactor fill [15], [16].

This study aims to bridge the gap between existing modeling approaches and their application in industry. This is done by exploring the potential of online measurements for model development, on the one hand, and by presenting model applications specifically tailored to enzyme production processes, on the other hand.

## METHODS AND MODELS

Three bioprocess models are used to discuss and explore the advantages of integrating novel online measurements into model development. All models are designed for the same industrial bioprocess, assuming substrate as the primary limiting factor for cell growth and death. Each model incorporates mass balances for key components, including reactor mass, biomass, substrate, product and dissolved oxygen. Due to confidential reasons, model parameters for each of the models cannot be disclosed.

A pure mechanistic model (model i) exhibits the highest dependency on offline data, requiring both CDW and offline rheology measurements. Essentially the model structure can be seen in Albeak et al., 2012 [6], with the difference being that yields have been linked to the growth rate, rather than being constant as well as the integration of a Monod growth kinetic.

Cell death is not modelled explicitly in model i. This decision reflects the limited precision of CDW measurements, which prevents robust estimation of death kinetics. The linear yields correlation as well as $\mu_{max}$ has been determined experimentally, whereas the remaining parameters were fitted using data from six fermentations covering the relevant operational space. Additionally, enzyme production is modelled based on a constant rate and includes a product inhibition term. The applied $k_La$ correlation is presented in equation 1.

$$k_La = C * \left(\frac{P}{V}\right)^a * v_s^b * \mu_{app}^c \quad (1)$$

The apparent viscosity is described using the Henzler and Otto model in which the power-law parameters are fitted to rheological measurements, as presented in Albeak et al., 2012 [6].

The only distinction between the mechanistic model (model i) and the second model, model ii, is that the apparent viscosity is replaced by online viscosity. In this approach, the $k_La$ correlation, shown in equation 2, includes online viscosity that is predicted by a supervised LGBM machine learning (ML) model, resulting in a sequential hybrid model. The ML model, trained with 27 historical fermentation processes from pilot plant and production, utilizing different fungal strains, predicts the online viscosity based on mechanistic modelled input features, as described in more detail in [17].

$$k_La = C * \left(\frac{P}{V}\right)^a * v_s^b * \mu_{online}^c \quad (2)$$

Therefore, model ii advances model i by increasing the use of online data (i.e. viscosity), while model iii builds upon model ii by integrating additional online measurements (i.e. capacitance), consequently reducing the need for offline sampling. The availability of online viable cell concentration measurements enables model iii to explicitly incorporate cell-growth and cell-death kinetics, both formulated as functions of substrate concentration and dissolved oxygen levels [18].

In addition, model iii integrates an extended ML–based viscosity model from model ii that includes capacitance as an input feature. However, this dataset consists of only two pilot-scale fermentation processes conducted with the same production strain. The restricted size of this dataset reflects the current limited availability of fermentation batches, equipped with online capacitance probes.

Consequently, in contrast to model i and model ii, which model biomass growth with a Monod model, model iii, predicts the viable cell concentration with a Contois-type growth and O'Brien-type death kinetic [19], [20]. As this extension increases the number of kinetic parameters in model iii, a differential evolution algorithm is employed to ensure sufficient exploration of the enlarged parameter space. The optimization applied the `'best1bin'` strategy with a population size of 6 and a maximum of 30 generations as well as a relaxed tolerance of 0.01 to enable early termination when improvement falls below 1% [21].

Due to limitations in the availability of offline and online biomass and rheology measurements, it was not possible to obtain a sufficiently comprehensive data set to calibrate all models on the same dataset, resulting in the use of the two data sets. Model i and ii are calibrated

on six 550L fermentation processes designed to explore the operational space of the system. In contrast, model iii is based on two 550L fermentations with different designs, one targeting three specific growth rates, while the other examines cell behavior under varying $k_L a$ conditions. The presented results are validated on additional fermentation processes at pilot and large scale that were not used for calibrating the models.

## Cost optimization

In-silico cost optimization of a fermentation process using a comprehensive bioprocess model represents a compelling application of modeling for industrial purposes [22].

The first step of a cost optimization involves linking the relevant cost factors, as listed in Table 1, to the simulation. For the purposes of this study, and due to the limited cost information available in the literature, we assumed a fixed baseline operating cost, denoted as fixed overhead costs. These represent expenses that occur regardless of how the fermentation is run. The values are based on internal company data and cannot be disclosed.

Other costs are associated with either the reactor start or end filling, the inherent process operating conditions as well as the fermentation time.

The energy prices in the analysis are based on historical data from the Danish energy market and reflect the minimum, maximum and average price over the last 10 years [23]. The other costs are based on literature values selected to best approximate the present case; however, the availability of detailed information in the literature is rather limited [16], [24], [25].

**Table 1:** Cost factors of a fermentation process

| | | |
|---|---|---|
| **Fixed Costs** | fixed overhead costs | confidential |
| **Variable Costs** | Electricity | 0.8, 1.8, 2.8 [23] [DKK/kwh] |
| | Carbon source | 4.23 [16] [DKK/kg] |
| | Ammonia | 1.94 [16] [DKK/kg] |
| | Media | 0.26 [24] [DKK/kg] |
| | Recovery Cost | 4.49 [25] [DKK/kg] |

In the second step, a realistic manufacturing scenario is embedded within the optimization problem. The problem is formulated as a nonlinear, simulation-based, single-objective constrained optimization problem. The decision variables $\mathbf{x} = [\mathrm{p}, \mathrm{a}, \mathrm{g}, \mathrm{t_f}]^{\mathrm{T}}$, represents pressure, aeration, agitation, and fermentation time. The objective is to minimize the total fermentation cost $\mathrm{C}(\mathbf{x})$, subject to meet a required enzyme production $\mathrm{P}(\mathbf{x}) \geq \mathrm{P_{target}}$ and respecting operational bounds $\mathrm{x_i^{min}} \leq \mathrm{x_i} \leq \mathrm{x_i^{max}}$, represented in the following formulation.

$$\min_{x} C(x),$$

$$s.t.\, P(\boldsymbol{x}) \geq P_{target},$$

$$x_i^{min} \leq x_i \leq x_i^{max}, i \in \{p, a, g, t_f\}$$

A nested root-finding procedure adjusts the initial reactor fill to ensure identical final fill levels across all simulations. Because the model exhibits non-linear, non-convex behavior without analytical gradients, the optimization is solved using a Genetic Algorithm with a population size of 50, up to 25 generations, using tournament selection, two-point crossover (probability 0.5), and Gaussian mutation (probability 0.5). The optimization process is initiated by generating 50 initial points within the design space using Latin Hypercube Sampling (LHS) [26].

## Advanced control for the reactor end fill

Many industrial enzyme production processes have already been extensively optimized, including by adjusting the feed rates to maintain a stable oxygen balance. However, as this normally leads to varying reactor end fills, a subsequent objective might be to reliably hit a defined end fill. Reactor end fills are linked to the total product produced and beyond that enhances manufacturing planning reliability by reducing process deviations. Model predictive control (MPC) is widely regarded as a powerful approach to enable such advanced control [6].

To reduce batch-to-batch variability and achieve this in DO-controlled fungal fermentation, a modular in-silico workflow that combines biased initial planning, real-time parameter adjustment, and constraint-based input optimization, is presented. First, a realistic model-process mismatch is created by distorting a calibrated "source" process model: the dynamic substrate and oxygen yields are influenced by a constant factor that is randomly determined in the range of ±30% of the yield's value. Using this deliberately distorted model, a Brent root-finding optimization is employed to determine the initial reactor fill that would result in the fermentation reaching the predefined final reactor fill. That start fill is applied to the unperturbed source (or truth) model to generate synthetic batch data, representing the realized process.

During the run, the algorithm corrects the distorted model at specified control points by finding correction factors for the dynamic yields, using the available online data of viable cell concentration, oxygen uptake rate (OUR), and feed rate by minimizing a normalized mean-squared error over the time to the checkpoint with Nelder-Mead under conservative tolerances. Normalization guards against misalignment and scale differences and regularization with constraints keeps parameters physically plausible. The corrected model is then rolled forward to forecast the rest of the batch. If the predicted

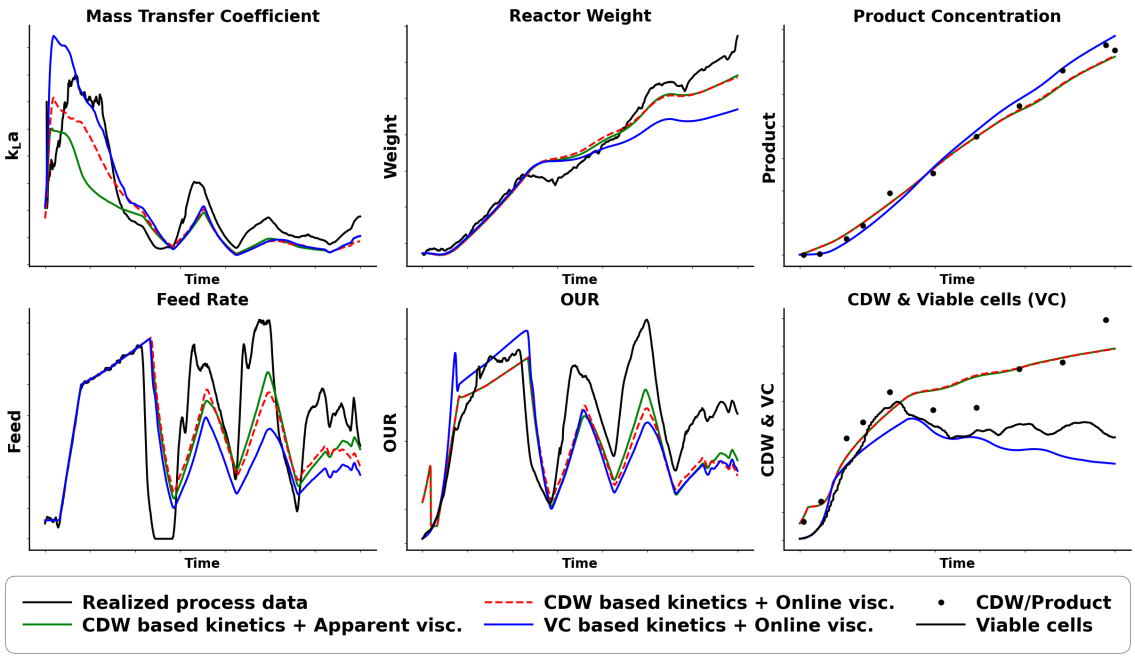


**Figure 1.** Pilot-scale predictions for the three models.

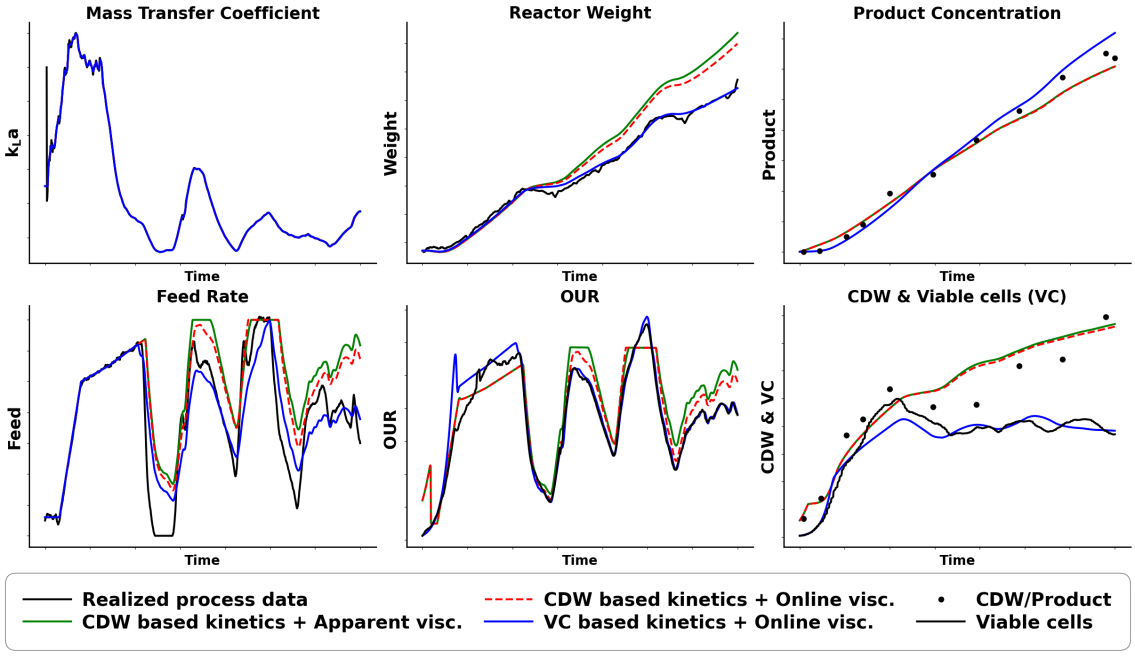


**Figure 2.** Pilot-scale predictions for the three models with realized $k_L a$.

end fill based on the new model deviates from the target beyond a threshold of e.g. ±1%, a bounded L-BFGS-B adjusts the agitator speed and aeration. This approach is possible, as with a DO-controlled process, there is a direct correlation between the OTR and the final reactor fill of a process.

$$Agitation\ and\ Aeration \uparrow \rightarrow OTR \uparrow \rightarrow DO \uparrow \rightarrow feed\ rate \uparrow \rightarrow end\ fill \uparrow$$

By adjusting the agitator speed and aeration under DO-controlled settings, a DO concentration close to the set point as well as a final fill that corresponds to the desired final fill of the process is ensured. This can be achieved by optimizing both the agitation and the

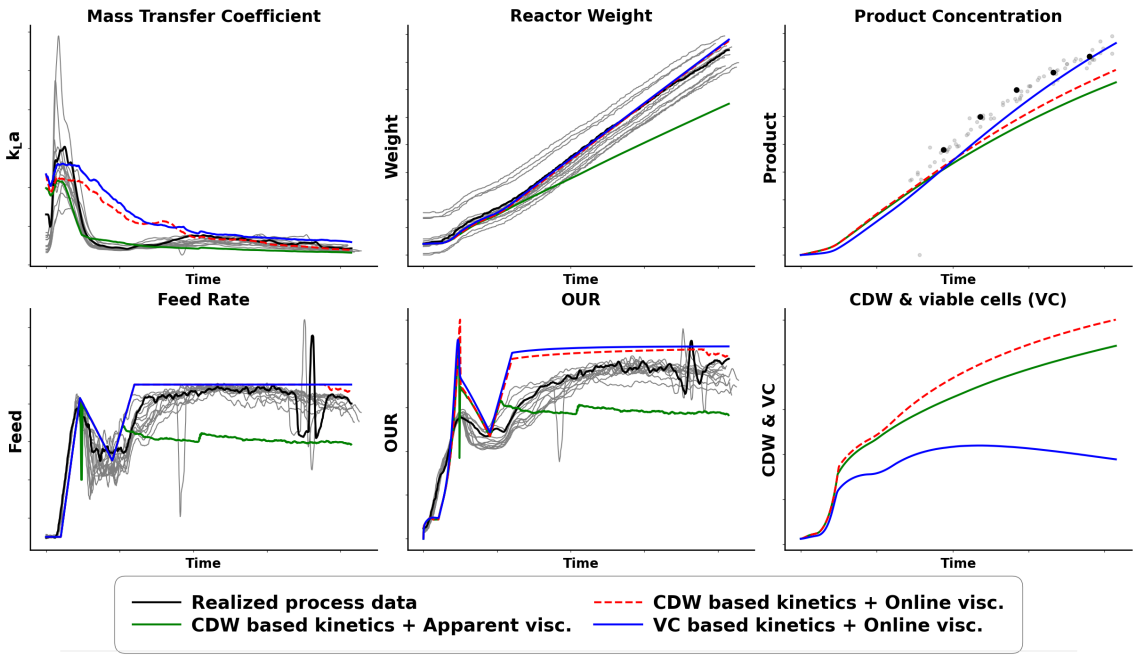


**Figure 3.** Large-scale predictions for the three models.

aeration based on the squared error between the final reactor fill prediction of the corrected model and the target fill using an L-BFGS-B optimization algorithm with moderate tolerances.

After executing this framework at each checkpoint, all actions are logged and saved, as they define the process until the next checkpoint. This fit-predict-control loop repeats to batch completion, maintaining robust DO control while steering the process to the target end fill under initial model inaccuracy. To reduce the computational cost, the framework is only activated at those time points, in which the modelled predictions deviate from the actual realized process data.

# RESULTS

## Model simulation for pilot and large scale

Figure 1 presents the closed-loop simulation results for models i, ii, and iii. The empirical $k_La$ models, each depending on their respective biological and physical sub-models, show reasonable agreement with the measured data throughout most of the fermentation process. Deviations in the predicted $k_La$ values occur primarily during the initial hours and can largely be attributed to viscosity effects. These early-phase differences arise either from the use of different viscosity models or from discrepancies in the biological sub-models implicitly embedded in the $k_La$ estimation.

Because the process is intentionally operated at its maximum feed rate during the initial hours, the early differences in $k_La$ do not translate into additional feed addition. As the predicted $k_La$ converges for the remainder of the fermentation, and because model i and ii share similar underlying biological sub-models, the resulting state predictions overlap for most variables during the closed-loop pilot-scale validation run.

Model iii, which was developed using only two fermentation datasets and viable cell measurements, underestimates the reactor fill compared to the observed data. Further investigation is required to understand the root causes of the discrepancies among the models. One possible diagnostic approach is to rerun the simulations using the realized $k_La$ profile, effectively decoupling the physical mass-transfer model. This allows a focused assessment of the biological sub-models' accuracy, as illustrated in Figure 2.

Figure 2 shows that the biological sub-models in models i and ii systematically result in an overprediction of the reactor mass when the realized $\mathrm{k_La}$ profile is imposed. In contrast the biological sub-model in model iii lead to an accurate prediction of the reactor mass. This indicates that, for models i and ii, inaccuracies in the physical $\mathrm{k_La}$ model and the biological growth model partially cancel each other out, leading to an apparently improved mass prediction in the fully coupled simulation. In contrast, the biological sub-model of model iii seems to be more accurate but does not benefit from this compensatory effect. Therefore, model iii suffers more directly from the limitations of the $\mathrm{k_La}$ model, when it's simulated.

Figure 3 illustrates the performance of the same models at production scale, compared against multiple manufacturing datasets shown in grey, with the black

trajectory representing the specific batch, which operational settings are used as input for the simulation.

Unlike the pilot-scale scenario, the $k_La$ predictions at large scale do not align well with the observed data. This mismatch indicates the limitations of the empirical $k_La$, developed at pilot scale and employed at production scale. Because of these challenges, there might be the need for either re-calibration at production scale or a theoretically grounded $k_La$ model that can scale effectively from pilot to production.

Since the hybrid models generally overpredict $k_La$, the process operates at its maximum feed ramp due to the DO-control, whereas the purely mechanistic model underpredicts $k_La$, resulting in a reduced feed rate and deviations in both reactor fill and product predictions. No biomass measurements are available due to limited availability at production scale.

Overall, the results demonstrate that capacitance measurements, enables the development of a more accurate and realistic biological model at pilot scale. In contrast, integrating online viscosity data does not lead to a noticeable improvement in prediction accuracy for this case, but it also does not negatively affect the physical $k_La$ model. Combined with the advantage that both, capacitance and online viscosity reduce the need for frequent offline sampling, these findings highlight the value utilizing online data for model development.

## Cost optimization

Cost optimization was carried out using model ii at a pilot scale, as it is known from previous work that this model provides so far, the most robust and broadly applicable predictions [17]. This is essential for such a cost optimization analysis in which a wide range of operational conditions are evaluated. The primary objective is to minimize the overall campaign cost under specific constraints as elaborated in the method section.

Due to confidentiality constraints, the results in these sections are presented in relative terms. Accordingly, the individual cost factors of a fermentation process in Table 2 are shown as percentages of the total fermentation cost. This allows identification of each factor's contribution under different electricity price scenarios. The analysis of Table 2 reveals that as electricity prices increase, the share of electricity costs rise substantially, from 12.4% for 0.8 DKK/kWh to 24.9% for 2.8 DKK/kWh, which is expected. Consequently, the relative contribution of other cost factors decreases. This trend aligns well with the general understanding of cost distribution in fermentation processes: at lower electricity prices, recovery, substrate and fixed costs dominate, whereas at higher prices, electricity contributes more than substrate alongside recovery and fixed costs.

**Table 2:** Individual fermentation cost factors at each electricity price, scaled by the corresponding total fermentation cost.

| **Electricity [DKK/kWh]** | **0.8** | **1.8** | **2.8** |
|---|---|---|---|
| **Starting costs [%]** | 2.2 | 2.2 | 2 |
| **Electricity [%]** | 12.4 | 18 | 24.9 |
| **Substrate [%]** | 17.3 | 13.9 | 12.7 |
| **Ammonia [%]** | 1.9 | 1.5 | 1.4 |
| **Recovery [%]** | 56.6 | 55 | 50.4 |
| **Fixed costs [%]** | 9.6 | 9.3 | 8.6 |

Table 3 lists the process decision variables $x$ across the three electricity price scenarios. The decision variables $x$ in Table 3 are normalized by their respective upper bound $x_i^{\max}$, providing insights into how intensively each decision variable is utilized. Interestingly, fermentation time remains nearly constant across all cases. Pressure is found at approximately 93% of its maximum value for the low electricity scenario and increases to almost 99% under higher electricity prices, which is consistent with its low-cost impact on the process. Higher headspace pressure reduces evaporation by lowering the vapor liquid driving force, thereby influencing the water balance and indirectly affecting the mass-based calculations [15].

In contrast, energy-intensive parameters such as agitation and aeration are significantly reduced. For example, aeration starts at about 100% for 0.8 DKK/kWh but drops to around 60% for 1.8 and 2.8 DKK/kWh. Agitation already starts with 60% utilization of $x_i^{\max}$ for the low energy cost scenario and drops to 50% for the higher energy costs, which also aligns with the overall expectations, as those decision variables are directly linked to higher electricity costs.

**Table 3:** Optimized decision variables $x$, scaled by their corresponding upper limit $x_i^{\max}$ .

| **Electricity [DKK/kWh]** | **0.8** | **1.8** | **2.8** |
|---|---|---|---|
| **Aeration [%]** | 100 | 61.6 | 61.4 |
| **Agitation [%]** | 60.7 | 52.8 | 51.8 |
| **Pressure [%]** | 92.7 | 95.5 | 98.8 |
| **Fermentation time [%]** | 81.8 | 81.8 | 82.1 |

Finally, the results in Table 4 and Figure 4 are scaled relative to the cost associated with a reasonable current industrial standard fermentation, defined as operating all decision variables $x$ at their respective upper limits $x_i^{\max}$, as implied in [2], [3]. Table 4 summarizes the scenario-specific total campaign costs. The results indicate that rising electricity prices amplify the cost advantage of the optimized campaign relative to a strategy in which all operational variables are maintained at their maximum setpoints. E.g. at a price of 0.8 DKK/kWh, the optimized campaign costs only 80.5% of the cost of the campaign that would result from a typical current standard strategy.

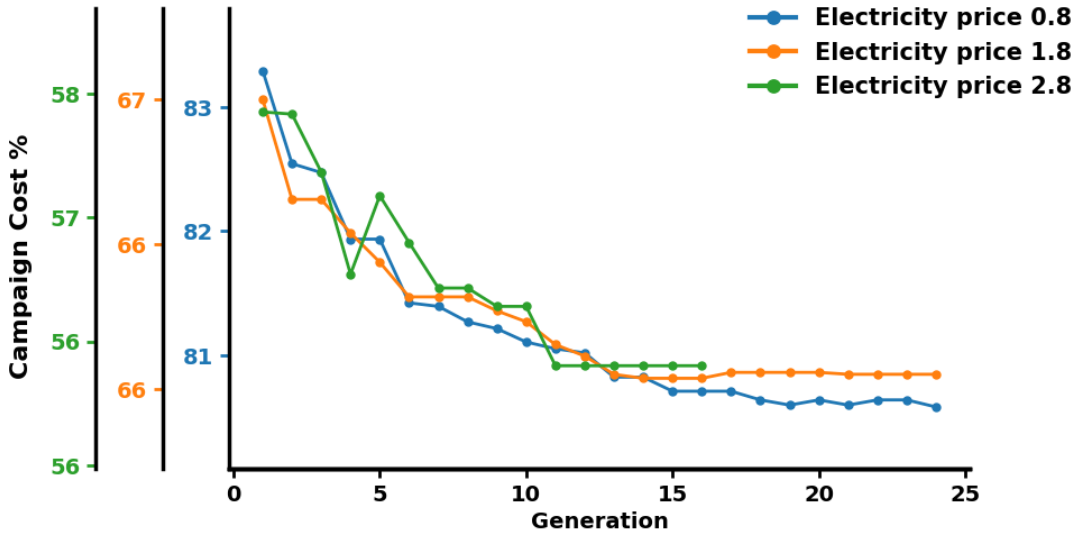


**Figure 4.** Campaign costs in percentage, scaled in the same manner as in Table 4.

**Table 4:** Total campaign costs for each electricity cost scenario, scaled by cost of a state-of-the-art operational strategy ($x_i = x_i^{max}$)

| **Electricity [DKK/kWh]** | **0.8** | **1.8** | **2.8** |
|---|---|---|---|
| **Total campaign costs [%]** | 80.5 | 65.6 | 56.3 |

Figure 4 illustrates the campaign cost progression across generations of the differential evolution algorithm, scaled in the same manner as the values in Table 4. The visualization reveals that for each electricity price scenario, the optimizer convergences and successfully identifies optimal process conditions within the given constraints. It also reveals that the optimization finds a very good first condition in the first generation of the optimization, which is likely caused by the broad initial LHS screening.

The study provides an example of how a bioprocess model can be used to evaluate the cost implications for different electricity price scenarios. The results reveal that operating all parameters at 100% ($x_i = x_i^{max}$) is not the most cost-efficient, which becomes increasingly evident as energy prices rise. Also, the results indicate that increasing energy prices primarily affect energy-intensive operations such as agitation and aeration, which should be scaled down to reduce costs, while pressure can remain near its maximum due to its negligible cost impact [16]. Interestingly, the comparison between 1.8 and 2.8 DKK/kWh shows minimal differences in the process conditions, suggesting a potential plateau in cost sensitivity beyond a certain threshold.

The optimization, performed at pilot scale, assumes constant values for agitation, aeration, and pressure throughout the fermentation process, which may not reflect the most efficient strategy in practice, but should be efficient enough for this purpose of energy cost evaluation. Furthermore, the results are considered to be highly dependent on the underlying model, scale and cost assumptions, limiting their generalizability to other processes. Future work could address time-dependent operational adjustments and include a broader range of electricity price scenarios to better capture system dynamics and identify potential tipping points for operational changes. Similar analysis at large scale might also be very interesting but first requires a similar broadly accurate process model . Finally, many more industrial relevant business cases can be approached using the same framework and subsequently customized for the specific application.

## Advanced control for the reactor end fill

Advanced control was implemented using the viable cell model (model iii), which offers the advantage of incorporating additional online measurements into the control strategy. To imitate a realistic scenario for MPC of an industrial fermentation process, the first step is to define a target reactor fill and perform an optimization to determine the required initial fill, which has been done with the same procedure as for the cost analysis. This analysis was executed using a distorted process model to create a discrepancy between the model and the process, as might occur in a real case.

The mimicked fermentation process, implemented by using the correct model and initiated with the estimated start fill, is represented by the black trajectories in

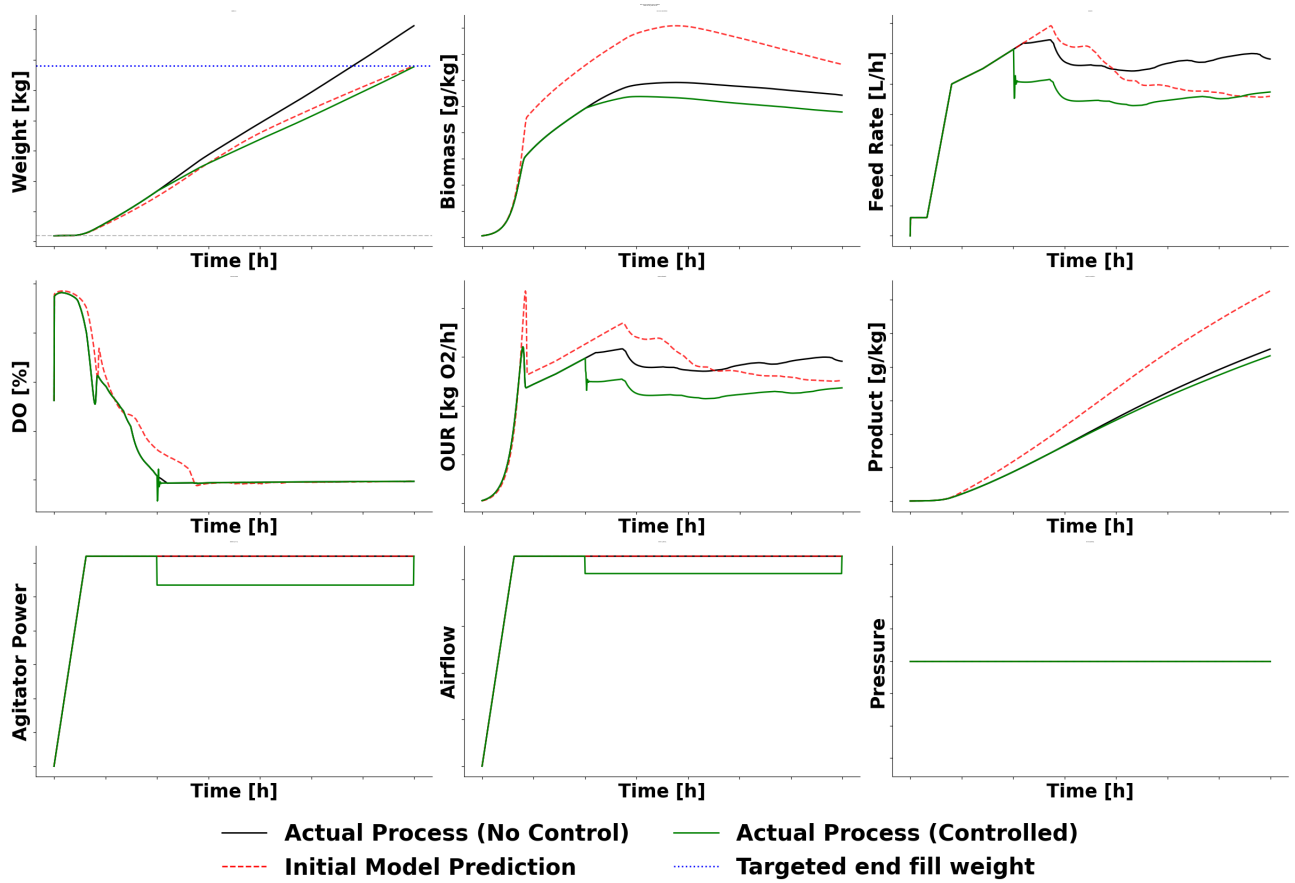


**Figure 5.** Full Fermentation process for the initial model and the synthetic process with and without advanced control.

Figure 5. As expected, without a corrective control mechanism, this leads to a reactor end fill that deviates from the defined end fill, underscoring the need for a corrective control strategy.

In contrast, the controlled fermentation process successfully reaches the target end fill. The optimizer adjusts agitation and aeration by lowering their setpoints, consequently reducing the DO-controlled feed rate and thus the final fill. The agitation is tuned a bit more than the aeration, which can be explained by the greater influence on the oxygen mass transfer. In addition, less aeration not only reduces the feed rate, but also evaporation, which lowers the total effect on the final weight.

Those results demonstrate the effectiveness of the control strategy described in the *Methods* section. Enabling sequential adjustments in which agitation and aeration are modified to achieve the desired final fill, while keeping DO close to its setpoint.

Under control, the final product concentration is slightly lower compared to the uncontrolled scenario and the initial model, reflecting the reduced feed addition and corresponding decrease in biomass concentration. Nevertheless, the reactor does not overfill, which is set as the main objective. This scenario illustrates that, even with an inaccurate initial model, the proposed framework can iteratively correct the model and control the process by fine-tuning agitation and aeration to ensure the process meets the end fill target without violating DO constraints.

Future work should focus on implementing and validating this approach in a real-world setting, which requires careful consideration. System boundary conditions, easily overlooked in simulations, could lead to operational failures if not properly addressed. These constraints must be incorporated into the simulation and thoroughly evaluated before deploying such a closed-loop model predictive control strategy in a pilot plant environment.

Additionally, attention must be given to the time intervals for evaluating control actions. These intervals should align with process dynamics and ideally exceed the time required by the computational framework to update the model, and adjust agitation, aeration and feed rate settings before the next evaluation point.

## CONCLUSION

This study first discusses the benefits of utilizing online rheology and online biomass measurements for fermentation models, emphasizing that especially the integration of capacitance data seems to improve the biological sub-model accuracy. Combined with the reduced labor associated with offline measurements, this supports the usage of online data to tackle the resource-intensive and time-consuming model development.

Secondly, the study demonstrates the applicability of bioprocess models tailored for industrial enzyme production, showing that electricity prices substantially influence the optimal operating strategy. The results clearly indicate that maximizing all decision variables, such as agitation, aeration, or fermentation time, is not cost-efficient under the given optimization problem and varying electricity prices. Finally, the in-silico MPC case illustrates that an initial model–process mismatch can be corrected in real time, enabling dynamic adjustment of agitation and aeration to ensure that the reactor achieves its target end-fill while maintaining DO control throughout the process.

## ACKNOWLEDGEMENTS

Special thanks to the entire team at the Novonesis fermentation pilot plant for their valuable involvement in this project

## AUTHOR IDENTIFIERS

Author ORCIDs:
ML: 0009-0006-6389-6563

## REFERENCES

1. P. Stanbury, A. Whitaker, and S. Hall, *Principles of fermentation technology*. Elsevier, 2013.
2. Villadsen J, Nielsen J, Lidén G. Bioreaction engineering principles. Springer US (2011). https://doi.org/10.1007/978-1-4419-9688-6
3. Doran PM. Reactor engineering. Bioprocess Engineering Principles :333-391 (1995). https://doi.org/10.1016/b978-012220855-3/50013-4
4. Rydal T, Frandsen J, Nadal?Rey G, Albæk MO, Ramin P. Bringing a scalable adaptive hybrid modeling framework closer to industrial use: application on a multiscale fungal fermentation. Biotech & Bioengineering 121:1609-1625 (2024). https://doi.org/10.1002/bit.28670
5. Albino M, Gargalo CL, Nadal-Rey G, Albæk MO, Krühne U, Gernaey KV. Hybrid modeling for on-line fermentation optimization and scale-up: a review. Processes 12:1635 (2024). https://doi.org/10.3390/pr12081635
6. Albaek MO, Gernaey KV, Hansen MS, Stocks SM. Modeling enzyme production with aspergillus oryzae in pilot scale vessels with different agitation, aeration, and agitator types. Biotech & Bioengineering 108:1828-1840 (2011). https://doi.org/10.1002/bit.23121
7. Kager J, Herwig C, Stelzer IV. State estimation for a penicillin fed-batch process combining particle filtering methods with online and time delayed offline measurements. Chemical Engineering Science 177:234-244 (2018). https://doi.org/10.1016/j.ces.2017.11.049
8. Pu Y, Chaudhry S, Parikh M, Berry J. Application of in-line viscometer for in-process monitoring of microcrystalline cellulose-carboxymethylcellulose hydrogel formation during batch manufacturing. Drug Development and Industrial Pharmacy 41:28-34 (2014). https://doi.org/10.3109/03639045.2013.845837
9. Bergin A, Carvell J, Butler M. Applications of biocapacitance to cell culture manufacturing. Biotechnology Advances 61:108048 (2022). https://doi.org/10.1016/j.biotechadv.2022.108048
10. Fehrenbach R, Comberbach M, Pêtre JO. On-line biomass monitoring by capacitance measurement. Journal of Biotechnology 23:303-314 (1992). https://doi.org/10.1016/0168-1656(92)90077-m
11. Konakovsky V, Yagtu A, Clemens C, Müller M, Berger M, Schlatter S, Herwig C. Universal capacitance model for real-time biomass in cell culture. Sensors 15:22128-22150 (2015). https://doi.org/10.3390/s150922128
12. Herwig C, Pörtner R, Möller J. Digital twins. Springer International Publishing (2021). https://doi.org/10.1007/978-3-030-71660-8
13. Udugama IA, Lopez PC, Gargalo CL, Li X, Bayer C, Gernaey KV. Digital twin in biomanufacturing: challenges and opportunities towards its implementation. Syst Microbiol and Biomanuf 1:257-274 (2021). https://doi.org/10.1007/s43393-021-00024-0
14. Mears L, Stocks SM, Albaek MO, Sin G, Gernaey KV. Mechanistic fermentation models for process design, monitoring, and control. Trends in Biotechnology 35:914-924 (2017). https://doi.org/10.1016/j.tibtech.2017.07.002
15. Mears L, Stocks SM, Albaek MO, Cassells B, Sin G, Gernaey KV. A novel model?based control strategy for aerobic filamentous fungal fed?batch fermentation processes. Biotech & Bioengineering 114:1459-1468 (2017). https://doi.org/10.1002/bit.26274
16. Ferreira RG, Azzoni AR, Freitas S. Techno-economic analysis of the industrial production of a low-cost enzyme using E. coli: the case of

recombinant ?-glucosidase. Biotechnol Biofuels 11: (2018). https://doi.org/10.1186/s13068-018-1077-0
17. M. Lemperle, P. Ramin, J. Kager, B. Cassells, S. Stocks, and K. V. Gernaey, “Hybrid bioprocess model towards the development of a digital twin for an industrial fermentation process, ” *ESCAPE 35: 35th European Symposium on Computer Aided Process Engineering 2025*, pp. 199–200, 2025.
18. Esener AA, Veerman T, Roels JA, Kossen NWF. Modeling of bacterial growth; formulation and evaluation of a structured model. Biotech & Bioengineering 24:1749-1764 (2004). https://doi.org/10.1002/bit.260240803
19. CONTOIS DE. Kinetics of bacterial growth: relationship between population density and specific growth rate of continuous cultures. Journal of General Microbiology 21:40-50 (1959). https://doi.org/10.1099/00221287-21-1-40
20. O'Brien CM, Zhang Q, Daoutidis P, Hu WS. A hybrid mechanistic-empirical model for in silico mammalian cell bioprocess simulation. Metabolic Engineering 66:31-40 (2021). https://doi.org/10.1016/j.ymben.2021.03.016
21. Abimbola M Enitan . Food processing optimization using evolutionary algorithms. Afr. J. Biotechnol. 10: (2011). https://doi.org/10.5897/ajb11.410
22. Wagner N, Bosshart A, Wahler S, Failmezger J, Panke S, Bechtold M. Model-based cost optimization of a reaction–separation integrated process for the enzymatic production of the rare sugar d-psicose at elevated temperatures. Chemical Engineering Science 137:423-435 (2015). https://doi.org/10.1016/j.ces.2015.05.058
23. Statista, “Denmark: Monthly wholesale electricity price.” Accessed: Jan. 13, 2026. [Online]. Available: https://www.statista.com/statistics/1271525/denmark-monthly-wholesale-electricity-price/
24. R. Davis *et al.*, “Process Design and Economics for the Conversion of Lignocellulosic Biomass to Hydrocarbons: Dilute-Acid and Enzymatic Deconstruction of Biomass to Sugars and Catalytic Conversion of Sugars to Hydrocarbons, ” Mar. 2015.
25. J. Wimble, R. Ashizawa, and E. W. Swartz, “Analysis of the economic viability and environmental impacts of a conceptual process model for the recovery of lactic acid from spent media in cultivated meat production, ” *Biotechnol. Prog.*, 2025, doi: 10.1002/btpr.70094.
26. R. Storn and K. Price, “Differential Evolution - A Simple and Efficient Heuristic for Global Optimization over Continuous Spaces, ” *Journal of Global Optimization*, vol. 11, no. 4, pp. 341–359, 1997, doi: 10.1023/A:1008202821328/METRICS.